Supplementary figures for:

Defective thyroid hormone transport to the brain leads to astroglial alterations

Marina Guillén-Yunta[1*], Ángel García-Aldea[1*], Víctor Valcárcel-Hernández[1], Ainara Sanz-Bógalo[1], Emma Muñoz-Moreno[2], Maria Gisele Matheus[3], Carmen Grijota-Martínez[1,4], Soledad Bárez-López[1], Ana Montero-Pedrazuela[1], Ana Guadaño-Ferraz[1]

1 Department of Neurological Diseases and Aging, Instituto de Investigaciones Biomédicas Sols-Morreale, Consejo Superior de Investigaciones Científicas (CSIC), Universidad Autónoma de Madrid (UAM), Madrid, Spain.

2 Magnetic Imaging Resonance Core Facility, Institut d'Investigacions Biomèdiques August Pi I Sunyer (IDIBAPS), Barcelona, Spain.

3 Department of Radiology and Radiological Science, Medical University of South Carolina, Charleston, SC, USA

4 Department of Cell Biology, Faculty of Biology, Universidad Complutense de Madrid, Madrid, Spain

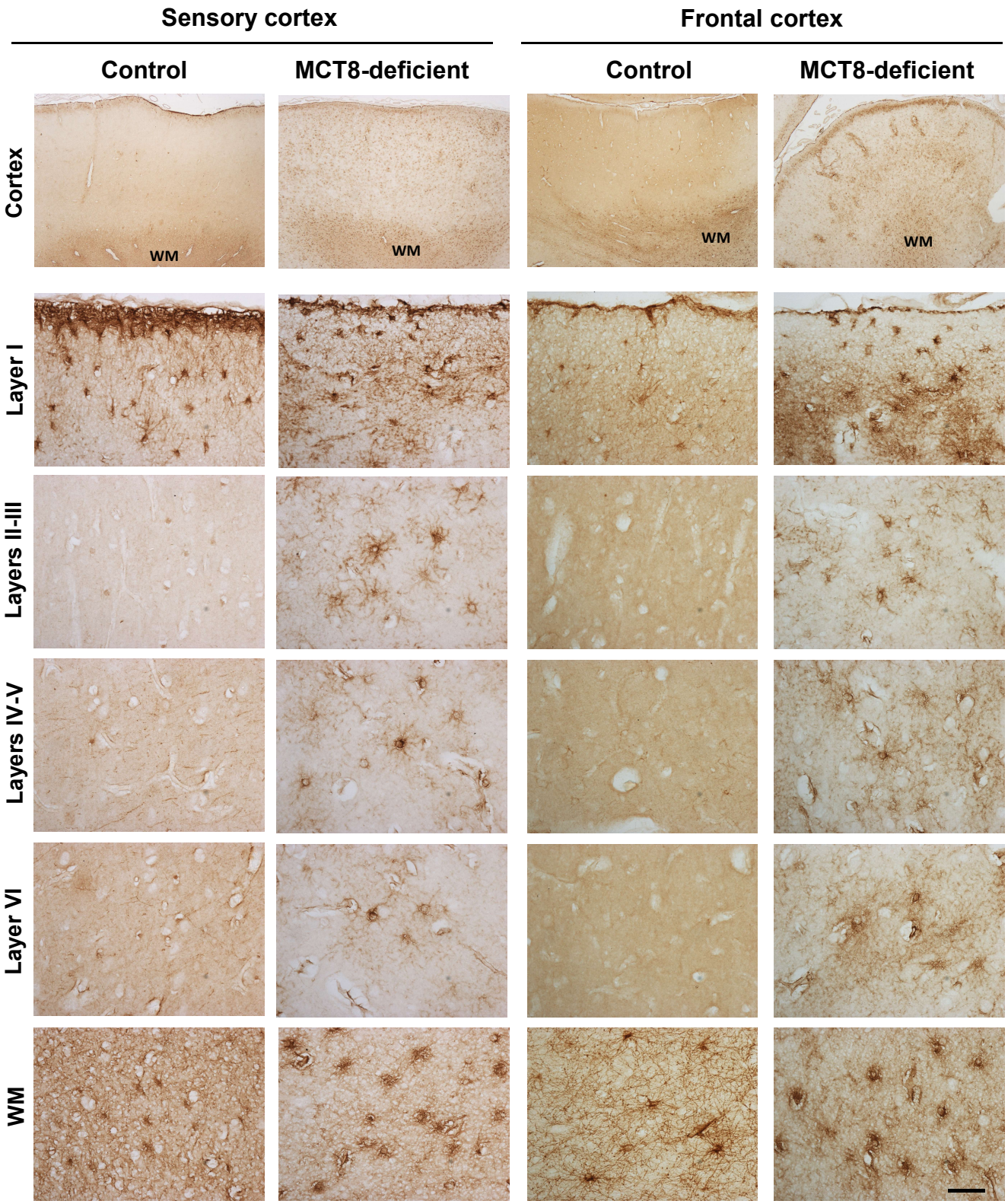

Supplementary Fig. 1 Expression of GFAP in the human sensory and frontal cortex. Expression of GFAP in the sensory cortex (left panels) and frontal cortex (right panels) of 12- and 10-year-old control subjects, respectively, and an 11-year-old MCT8-deficient subject. The upper panels show a panoramic view of the gyrus of the motor cortex, including all layers and the subcortical WM. Note the absence of staining in layers II-VI of the control samples and the widespread GFAP expression in the MCT8-deficient samples. The other panels show high-magnification images of different cortical layers and the subcortical WM. I-VI: layers of the motor cortex. WM: white matter. Scale bar: 1,000 µm in upper panels; 50 µm in other panels.

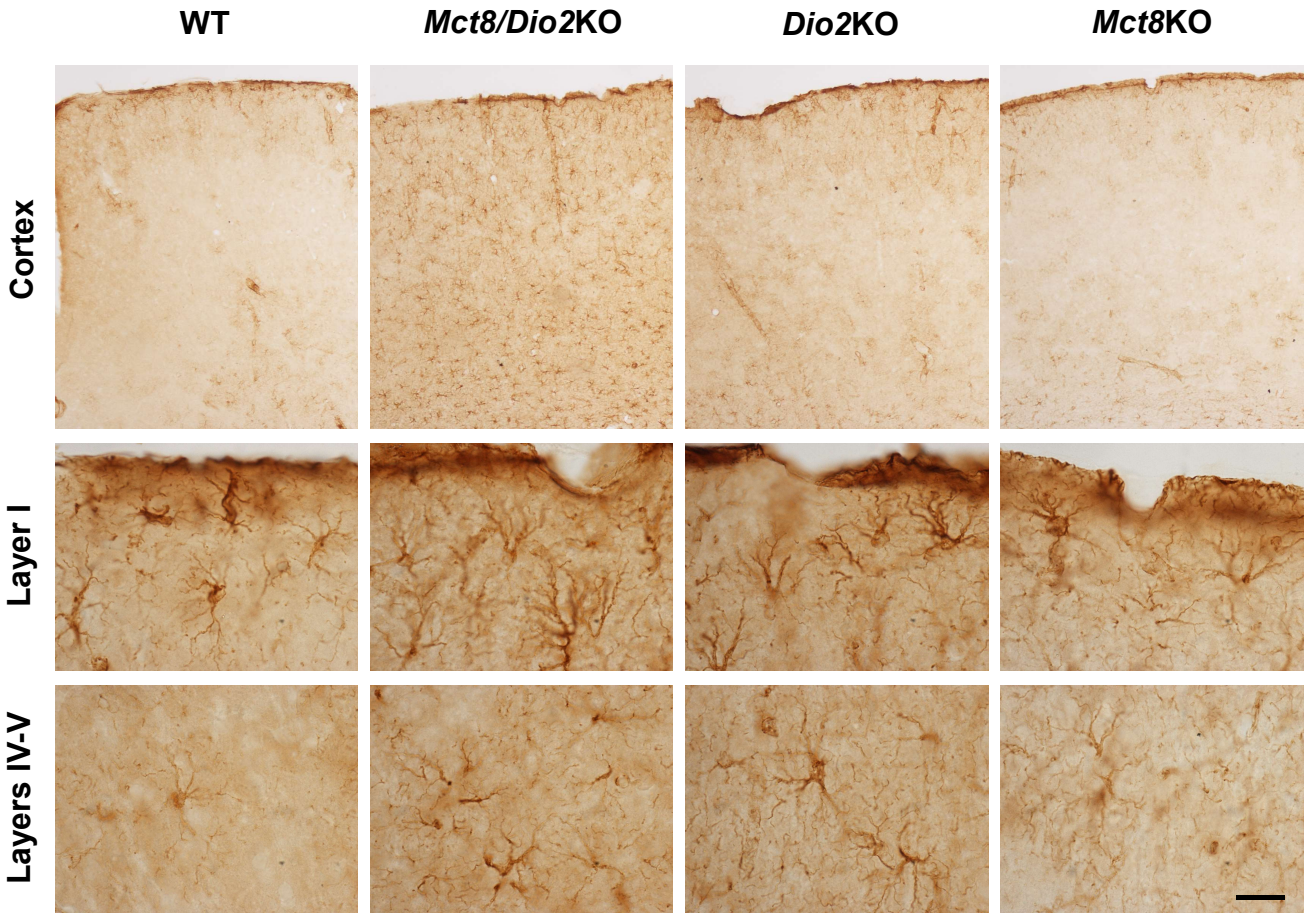

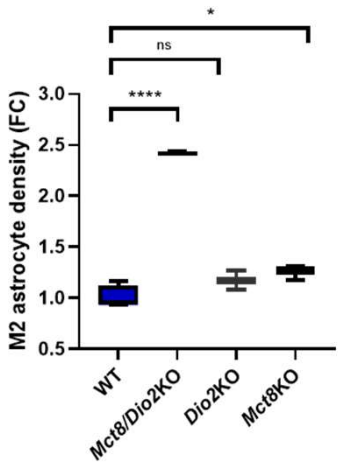

Supplementary Fig. 2 GFAP expression in the motor cortex of WT, *Mct8/Dio2*KO, *Dio2*KO, and *Mct8*KO mice. Analysis performed using 3-month-old WT, *Mct8/Dio2*KO, *Dio2*KO and *Mct8*KO mice (n=4 for each genotype). The upper panels show the general distribution pattern of GFAP+ astrocytes. Observe the increased expression of GFAP in astrocytes in the inner layers of the cortex in *Mct8/Dio2*KO and the intermediate phenotype of the single *Dio2*KO and *Mct8*KO mice. Higher magnification images show details in layer I and layers IV-V. Scale bar: 125 µm in upper panels; 20 µm in lower panels. Graph: quantitative analysis of the density of GFAP+ astrocytes in the M2 of animals of the four genotypes. *p< 0.05 and ****p < 0.0001 were determined by a two-tailed unpaired Student's t-test. M2: secondary motor cortex. FC: fold change.

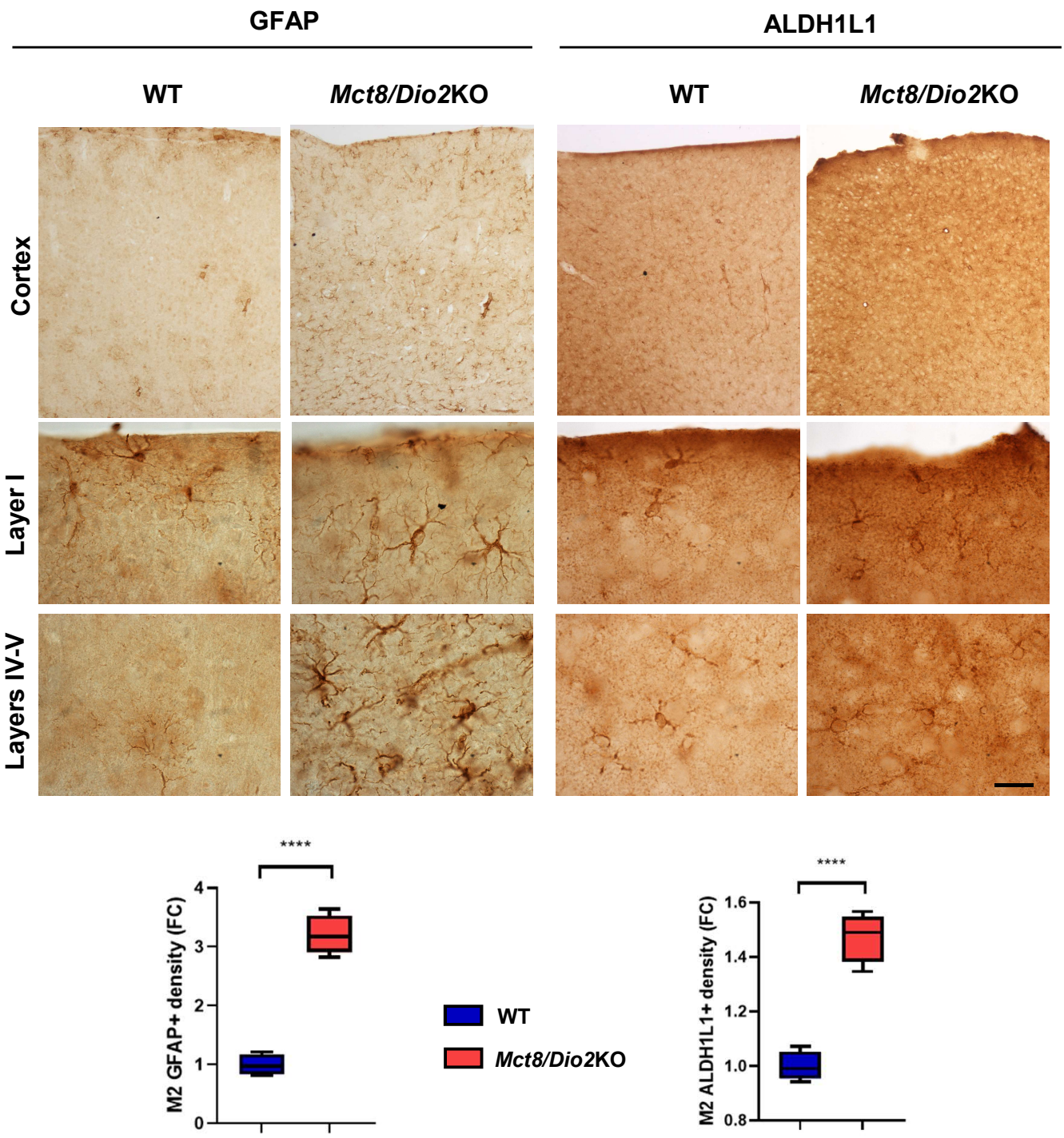

Supplementary Fig. 3 GFAP and ALDH1L1 expression in the motor cortex of 6-month-old WT and *Mct8/Dio2*KO mice. Analysis performed using WT (n=4) and *Mct8/Dio2*KO (n=4) mice. Left panels: GFAP expression. Right panels: ALDH1L1 expression. Upper panels show the general distribution pattern of GFAP+ and ALDH1L1+ astrocytes. Observe the different GFAP expression pattern in the inner layers of the cortex between both genotypes. Higher magnification images show details in layer I and layers IV-V. Scale bar: 125 µm in upper panels; 20 µm in lower panels. Graphs: quantitative analysis of the density of GFAP+ and ALDH1L1+ astrocytes in the M2 of WT (blue) and *Mct8/Dio2*KO (red) mice. ****$p < 0.0001$ was determined by a two-tailed unpaired Student's t-test. M2: secondary motor cortex. FC: fold change.